

**SYNTHESIS, OPTICAL, ELECTRICAL AND
CATALYTIC PROPERTIES OF
TITANIUM-BASED OXIDES MATERIALS AND
THEIR SODIUM-DOPED DERIVATIVES**

CHEW KER YIN

UNIVERSITI SAINS MALAYSIA

2016

**SYNTHESIS, OPTICAL, ELECTRICAL AND
CATALYTIC PROPERTIES OF TITANIUM-
BASED OXIDES MATERIALS AND THEIR
SODIUM-DOPED DERIVATIVES**

by

CHEW KER YIN

**Thesis submitted in fulfillment of the requirements
for the degree of
Doctor of Philosophy**

January 2016

ACKNOWLEDGEMENTS

Firstly, I would like to take this opportunity to thank my supervisor, Prof. Mohamad Abu Bakar and my co-supervisor, Dr Noor Hana Hanif Abu Bakar for their guidance and advice given throughout this work. I also thank Dr. Tan Wei Leng for useful comments and discussion during the writing up of this thesis.

I would also like to take this chance to thank Miss Jamilah and Mr. Johari from Electron Microscope and Microanalysis Department for their helps. A special thank for Mr. Mustakim from XRD Powder Crystallography for his assistance in operating XRD instrument. I am indebted to all the staffs in School of Chemical Sciences, Mr. Ali, Mr. Megat, Mr. Burhanuddin, Mrs Ami and Mr. Siva for their help in completing this work.

I would also like to express my gratitude for the financial support from Universiti Sains Malaysia (USM) and fellowship.

Last but not least, I would also like to thank my friends and family for giving me support and encouragement for finishing this work.

TABLE OF CONTENTS

	Page
ACKNOWLEDGEMENT	ii
TABLE OF CONTENTS	iii
LIST OF TABLES	viii
LIST OF FIGURES	ix
LIST OF ABBREVIATIONS	xiv
LIST OF SYMBOLS	xv
ABSTRAK	xvii
ABSTRACT	xix
CHAPTER 1-INTRODUCTION	
1.1 A Brief Overview	1
1.2 Problem Statements	3
1.3 Research Objectives	4
1.4 Scope of Study	4
1.5 Thesis Layout	5
1.6 References	7
CHAPTER 2-LITERATURE REVIEWS	
2.1 Overview of Metal Oxides	8
2.2 Surface of Metal Oxides	8
2.3 Titanium-Based Oxides	11
2.4 Synthesis Methods for Titanium-Based Oxides	13
2.4.1 Physical Methods	13

2.4.1.1 Solid State Milling Method	13
2.4.2 Wet Chemical Methods	14
2.4.2.1 Sol-Gel Method	14
2.4.2.2 Hydrothermal Method	17
2.4.2.3 Water-in-oil/Microemulsions Method	18
2.4.2.4 Polymerizing-Complexing Sol-Gel Method (Pechini Method)	20
2.5 Polymer-Inorganic Composites	20
2.5.1 Polymer/Metal or Metal Oxides Composites	20
2.5.2 Polymer/Titanium-Based Oxides Composites	21
2.5.3 PVA/Titanium-Based Oxides Composites	22
2.6 Applications of Titanium-Based Oxides	23
2.6.1 Catalysts for Transesterification	23
2.6.1.1 Titanium-Based Oxides	26
2.6.2 Electronic and Optical Applications	27
2.7 References	32
CHAPTER 3-EXPERIMENTAL	
3.1 Materials	43
3.2 Catalysis Study	43
3.2.1 Preparation of Catalysts	43
3.2.1.1 Synthesis of Barium Titanate (BaTiO_3)	43
3.2.1.2 Synthesis of Barium Nickel Titanate ($\text{Ba}_2\text{NiTi}_5\text{O}_{13}$)	44
3.2.1.3 Preparation of Na-doped TiO_2	45
3.2.1.4 Preparation of Na-doped BaTiO_3	45

4.3.3 Characterization of Na-doped Ba ₂ NiTi ₅ O ₁₃	79
4.3.4 Surface Morphology	82
4.3.5 BET Surface Analysis	89
4.3.6 Basicity Analysis	94
4.4 Summary	95
4.5 References	97

**CHAPTER 5-STRUCTURAL, THERMAL, ELECTROCHEMICAL AND
OPTICAL PROPERTIES OF PVA BASED POLYMER
COMPOSITES USING TiO₂, BaTiO₃ AND Ba₂NiTi₅O₁₃ AND
THEIR NA-DOPED ANALOGUE AS FILLERS**

5.1 Introduction	100
5.2 Preparation and Characterization	101
5.2.1 Phase Composition	101
5.2.2 Complexation Interaction	103
5.3 Thermal Study of PVA Composites	106
5.4 Electrical Conductivity	110
5.4.1 Effect of Fillers Loading	110
5.4.2 Effect of Na doping	116
5.5 Optical Properties	118
5.5.1 Effect of Fillers Loading	118
5.5.2 Effect of Na Doping	123
5.6 Summary	124
5.7 References	126

**CHAPTER 6-TiO₂, BaTiO₃ AND Ba₂NiTi₅O₁₃ AND THEIR Na DOPED
DERIVATIVES AS HETEROGENEOUS CATALYSTS IN
TRANSESTERIFICATION**

6.1 Introduction	130
6.2 Characterization of Methyl Esters	132
6.3 Optimization of Catalytic Parameters for Transesterification Palm Cooking Oil Using TiO ₂ , BaTiO ₃ and Ba ₂ NiTi ₅ O ₁₃	133
6.3.1 Effect of Oil to Methanol Volume Ratio	133
6.2.2 Effect of Catalyst Loading	135
6.2.3 Effect of Autoclaved Temperature	137
6.2.4 Effect of Autoclaved Duration	139
6.2.5 Transesterification of Palm Cooking Oil Using Na-Doped TiO ₂ , BaTiO ₃ and Ba ₂ NiTi ₅ O ₁₃ at Optimum Conditions	140
6.3 Summary	142
6.4 References	144

CHAPTER 7-CONCLUSIONS

7.1 Conclusions	146
7.2 Recommendations for Future Work	148

LIST OF PUBLICATIONS AND PRESENTATIONS AT CONFERENCES	149
--	-----

LIST OF TABLES

	Page
Table 4.1: BET surface area, pore sizes and pore volume of titanium-based oxides.	91
Table 4.2: Basicity of titanium-based oxides tested using Hammett indicators.	95
Table 5.1: FTIR peak assignments of PVA composites.	105
Table 5.2: Summary of thermal property of PVA composites.	109
Table 5.3: Summary of conductivity of PVA composite thin films with various weight ratios.	112
Table 5.4: Summary of conductivity of PVA/Na-TiO ₂ , PVA/Na-BaTiO ₃ and PVA/Na-Ba ₂ NiTi ₅ O ₁₃ composite thin films with various mole ratios.	117
Table 5.5: Summary of band gaps of PVA composites.	121
Table 6.1: Fatty acid composition.	132

LIST OF FIGURES

	Page
Figure 2.1: Schematic surface of metal oxide catalyst.	10
Figure 2.2: Perovskite crystal structure.	12
Figure 2.3: Schematic diagram of sol-gel method.	16
Figure 2.4: Nucleation and growth of particles.	18
Figure 2.5: Schematic diagram of microemulsion.	19
Figure 2.6: Chemical structure of PVA.	23
Figure 2.7: Schematic diagram representation of energy band gap of (a) insulator, (b) semiconductor and (c) metal.	28
Figure 2.8: Direct and indirect band gap.	29
Figure 2.9: Deformation of crystal structures of dielectrical barium titanate and thus the formation of net dipole moment.	31
Figure 4.1: XRD diffractograms of (a) as-prepared gel BaTiO ₃ and the BaTiO ₃ calcined at (b) 850 °C for 1 hour, (c) 900 °C for 1 hour, (d) 900 °C for 4 hours and (e) 900 °C for 5 hours.	54
Figure 4.2: FTIR spectra of (a) as-prepared gel BaTiO ₃ and the BaTiO ₃ calcined at (b) 850 °C for 1 hour, (c) 900 °C for 1 hour, (d) 900 °C for 4 hours and (e) 900 °C for 5 hours.	57
Figure 4.3: (a) Typical SEM micrograph (magnification 20000 times) of BaTiO ₃ calcined at 900 °C for 5 hours with (b) EDX spectra of calcined BaTiO ₃ .	59
Figure 4.4: XRD diffractograms of (a) as-prepared gel of Ba ₂ NiTi ₅ O ₁₃ and the Ba ₂ NiTi ₅ O ₁₃ calcined at 900 °C for (b) 4 and (c) 8 hours.	63

Figure 4.5:	FTIR spectra of (a) as-prepared gel of $\text{Ba}_2\text{NiTi}_5\text{O}_{13}$, and $\text{Ba}_2\text{NiTi}_5\text{O}_{13}$ calcined at 900 °C for (b) 4 hours and (c) 8 hours.	65
Figure 4.6:	(a) Typical SEM micrograph (magnification 20000 times) of $\text{Ba}_2\text{NiTi}_5\text{O}_{13}$ calcined at 900 °C for 8 hours with (b) EDX spectra of $\text{Ba}_2\text{NiTi}_5\text{O}_{13}$.	67
Figure 4.7:	XRD diffractograms of (a) TiO_2 and Na- TiO_2 doped with (b) 0.1, (c) 0.2, (d) 0.3, (e) 0.5 and (f) 1.0 mol % of Na.	71
Figure 4.8:	FTIR spectra of (a) TiO_2 and Na- TiO_2 doped with (b) 0.1, (c) 0.2, (d) 0.3, (e) 0.5 and (f) 1.0 mol % of Na.	73
Figure 4.9:	XRD diffractograms of Na- BaTiO_3 doped with (a) 0.1, (b) 0.2, (c) 0.3, (d) 0.5 and (e) 1.0 mol % of Na.	75
Figure 4.10:	FTIR spectra of Na- BaTiO_3 doped with (a) 0.1, (b) 0.2, (c) 0.3, (d) 0.5 and (e) 1.0 mol % of Na.	78
Figure 4.11:	XRD diffractograms of Na- $\text{Ba}_2\text{NiTi}_5\text{O}_{13}$ doped with (a) 0.1, (b) 0.2, (c) 0.3, (d) 0.5 and (e) 1.0 mol % of Na.	80
Figure 4.12:	FTIR spectra of Na- $\text{Ba}_2\text{NiTi}_5\text{O}_{13}$ doped with (a) 0.1, (b) 0.2, (c) 0.3, (d) 0.5 and (e) 1.0 mol % of Na.	81
Figure 4.13:	SEM micrographs of (a) undoped and (b) 0.1, (c) 0.2, (d) 0.3, (e) 0.5 and (f) 1.0 mol % Na-doped TiO_2 magnified 10000 times.	83
Figure 4.14:	Na atomic % and particle sizes distribution upon Na doping on TiO_2 .	84
Figure 4.15:	SEM micrographs of (a) undoped, (b) 0.1, (c) 0.2, (d) 0.3, (e) 0.5 and (f) 1.0 mol % Na-doped BaTiO_3 magnified 10000 times.	86

Figure 4.16:	Na atomic % and particle sizes distribution upon Na doping on BaTiO ₃ .	87
Figure 4.17:	SEM micrographs of (a) undoped and (b) 0.1, (c) 0.2, (d) 0.3, (e) 0.5 and (f) 1.0 mol % Na-doped Ba ₂ NiTi ₅ O ₁₃ magnified 25000 times.	88
Figure 4.18:	Na atomic % and particle sizes distribution upon Na doping on Ba ₂ NiTi ₅ O ₁₃ .	89
Figure 4.19:	BET adsorption-desorption isotherm of TiO ₂ .	90
Figure 4.20:	BET adsorption-desorption isotherm of BaTiO ₃ .	92
Figure 4.21:	BET adsorption-desorption isotherm of Ba ₂ NiTi ₅ O ₁₃ .	93
Figure 5.1:	Typical XRD diffractogram of (a) PVA, (b) PVA/TiO ₂ (20:1 w/w), (c) PVA/Na-TiO ₂ (0.3 mol % Na-doped; 20:1 w/w), (d) PVA/BaTiO ₃ (20:1 w/w), (e) PVA/Na-BaTiO ₃ (0.3 mol % Na-doped; 20:1 w/w), (f) PVA/Ba ₂ NiTi ₅ O ₁₃ (20:1 w/w) and (g) PVA/Na-Ba ₂ NiTi ₅ O ₁₃ (0.3 mol % Na-doped; 20 w/w).	102
Figure 5.2:	Typical FTIR spectra of (a) PVA, (b) PVA/TiO ₂ (20:1 w/w), (c) PVA/Na-TiO ₂ (0.3 mol % Na-doped; 20:1 w/w), (d) PVA/BaTiO ₃ (20:1 w/w), (e) PVA/Na-BaTiO ₃ (0.3 mol % Na-doped; 20:1 w/w), (f) PVA/Ba ₂ NiTi ₅ O ₁₃ (20:1 w/w) and (g) PVA/Na-Ba ₂ NiTi ₅ O ₁₃ (0.3 mol % Na-doped; 20 w/w).	104
Figure 5.3:	Typical DSC curves of (a) PVA and (b) PVA/TiO ₂ with the weight ratios of PVA to filler 20:1 w/w.	106

Figure 5.4:	Typical Nyquist plots of (a) PVA; weight ratios of PVA/ fillers composites (b) 2000:1 with inset, (c) 400:1, (d) 200:1, (e) 40:1, and (f) 20:1.	110
Figure 5.5:	Typical equivalent circuit.	113
Figure 5.6:	Typical UV spectra of (a) PVA, (b) PVA/TiO ₂ (20:1 w/w), (c) PVA/Na-TiO ₂ (0.3 mol % Na-doped; 20:1 w/w), (d) PVA/BaTiO ₃ (20:1 w/w), (e) PVA/Na-BaTiO ₃ (0.3 mol % Na-doped; 20:1 w/w), (f) PVA/Ba ₂ NiTi ₅ O ₁₃ (20:1 w/w) and (g) PVA/Na-Ba ₂ NiTi ₅ O ₁₃ (0.3 mol % Na-doped; 20 w/w).	119
Figure 6.1:	Typical GC chromatogram of methyl esters.	132
Figure 6.2:	Effect of oil to methanol volume ratio using 5.0 wt/v % catalysts of (a) TiO ₂ , (b) BaTiO ₃ and (c) Ba ₂ NiTi ₅ O ₁₃ at 150 °C for 2 hours on transesterification ME yield %.	134
Figure 6.3:	Effect of catalyst of (a) TiO ₂ , (b) BaTiO ₃ and (c) Ba ₂ NiTi ₅ O ₁₃ loading (catalyst/oil weight/volume %) with oil to methanol volume ratio 1:12 at 150 °C for 2 hours on transesterification ME yield %.	136
Figure 6.4:	Effect of temperature using 5.0 wt/v % catalysts of (a) TiO ₂ , (b) BaTiO ₃ and (c) Ba ₂ NiTi ₅ O ₁₃ with oil to methanol volume ratio 1:12 for 2 hours on transesterification ME yield %.	138
Figure 6.5:	Effect of autoclaved duration using 5.0 wt/v % catalysts of (a) TiO ₂ , (b) BaTiO ₃ and (c) Ba ₂ NiTi ₅ O ₁₃ with oil to methanol volume ratio 1:12 at 150 °C on transesterification ME yield %.	140

Figure 6.6: Effect of Na doping on catalysts of (a) TiO_2 , (b) BaTiO_3 and 141
(c) $\text{Ba}_2\text{NiTi}_5\text{O}_{13}$ with oil to methanol volume ratio 1:12 at
150 °C for 2 hours on transesterification ME yield %.

LIST OF ABBREVIATIONS

AC	Alternating Current
BDDT	Brunauer, Diming, Diming, Teller classification
BET	Brunauer-Emmett-Teller
CPE	Constant Phase Element
DSC	Differential Scanning Calorimetry
DC	Direct Current
EIS	Electrochemical Impedance Spectroscopy
EDX	Energy Dispersive X-Ray Spectroscopy
FAME	Fatty Acid Methyl Esters
FID	Flame Ionization Detector
FTIR	Fourier Transform Infrared Spectroscopy
GC	Gas Chromatography
IUPAC	International Union of Pure and Applied Chemistry
JCPDS	Joint Committee on Powder Diffraction Standards
LED	Light-emitting Diode
ME	Methyl Esters
PL	Photoluminescence
PVA	Polyvinyl Alcohol
SEM	Scanning Electron Microscopy
UV-vis	Ultraviolet-visible
XRD	X-ray Diffraction

LIST OF SYMBOLS

A	Absorbance
α	Absorption Coefficient
N	Area of the Films
E_g	Energy Band Gap
H	Basic Strength using Hammett Indicator
k	Boltzman's Constant
R_b	Bulk Resistance
n	Capacitive Parameter of CPE
n	Nonbonding Electronic Transition
R_{ct}	Charge Transfer Resistance
σ	Conductivity
C	Constant of UV Absorption
ν	Frequency of Electromagnetic Wave
T_g	Glass-Transition Temperature
I_0	Intensity of Incident Light
I	Intensity of Transmitted Light
ΔH_m	Melting Heat Enthalpy
T_m	Melting Temperature
h	Planck's Constant
$\%X_c$	Relative Crystallinity
σ^*	Sigma Antibonding Electronic Transition
T	Temperature
x	Thickness of the Films
W	Warburg Impedance
k	Wave Vector

**SINTESIS, OPTIKAL, ELEKTRIKAL DAN SIFAT PEMANGKINAN
BAHAN-BAHAN OKSIDA BERASAS TITANIUM DAN PENGEDOP-
NATRIUM TERBITAN MEREKA**

ABSTRAK

Barium titanat (BaTiO_3) dan barium nikel titanat ($\text{Ba}_2\text{NiTi}_5\text{O}_{13}$) telah disintesis melalui kaedah sol-gel. Mekanisma pembentukan BaTiO_3 dan $\text{Ba}_2\text{NiTi}_5\text{O}_{13}$ telah dicadangkan. Kesan pengedopan natrium (Na) pada komposisi struktur dan morfologi permukaan bagi 3 oksida berasas titanium iaitu titanium dioksida (TiO_2), BaTiO_3 and $\text{Ba}_2\text{NiTi}_5\text{O}_{13}$ telah dikaji. Struktur-struktur fasa TiO_2 , BaTiO_3 dan $\text{Ba}_2\text{NiTi}_5\text{O}_{13}$ iaitu anatase, kubik dan monoklinik, masing-masing dikekalkan selepas pengedopan Na. Ini menunjukkan bahawa penggantian atom Na pada atom Ti adalah satu fenomena permukaan. Transformasi morfologi zarah-zarah pengedop-Na BaTiO_3 telah diperhatikan. Penunjuk Hammett menunjukkan bahawa pengedop-Na $\text{Ba}_2\text{NiTi}_5\text{O}_{13}$ mempunyai kebesan yang tertinggi. Daripada hasil analisa BET, pengedop-Na $\text{Ba}_2\text{NiTi}_5\text{O}_{13}$ menunjukkan luas permukaan spesifik yang tertinggi berbanding dengan pengedop-Na BaTiO_3 dan pengedop-Na TiO_2 . Aplikasi oksida berasas titanium tersebut sebagai pengisi dalam polivinil alkohol (PVA) telah dikaji. Ciri-ciri struktur, haba, elektrik dan optik bagi polimer-polimer komposit telah dikaji. Hasil pembelauan sinar-X (XRD) dan kalorimetri pengimbasan pembezaan (DSC) menunjukkan bahawa polimer-polimer komposit ini adalah bersifat semikristal dengan kawasan amorfus yang tinggi dan nilai T_g yang rendah. 0.3 mol % pengedopan Na pada PVA/ TiO_2 PVA/ BaTiO_3 dan PVA/ $\text{Ba}_2\text{NiTi}_5\text{O}_{13}$ menunjukkan nilai kekonduksian adalah 9.540×10^{-7} , 1.667×10^{-7} dan 2.401×10^{-8} S cm^{-1} masing-masing. Jurang jalur optik PVA-berasas polimer-polimer komposit menunjukkan bahawa mereka adalah semikonduktor. Jurang jalur optik teranjak kepada biru apabila jumlah muatan pengisi

ditingkatkan dan juga jumlah pengedopan Na ditingkatkan. Hasil sintesis TiO_2 , BaTiO_3 dan $\text{Ba}_2\text{NiTi}_5\text{O}_{13}$ dan hasil pengedop-Na analog mereka yang diperolehi ini juga dipergunakan sebagai pemangkin heterogen dalam proses transesterifikasi minyak masak kelapa sawit. Parameter-parameter optima diperolehi adalah 5.0 wt/v % muatan pemangkin, nisbah isipadu minyak kepada metanol sebanyak 1:12 dan masa tindakbalas selama 2 jam pada suhu $150\text{ }^\circ\text{C}$. Di antara pemangkin-pemangkin tersebut, pengedop-Na $\text{Ba}_2\text{NiTi}_5\text{O}_{13}$ menunjukkan % hasil metil ester (ME) yang tertinggi (96.0 %), manakala TiO_2 menunjukkan % hasil yang terendah (76.3 %). Nilai % hasil metil ester (ME) adalah dipengaruhi oleh tahap kebesan dan saiz liang pemangkin tersebut.

**SYNTHESIS, OPTICAL, ELECTRICAL AND CATALYTIC PROPERTIES
OF TITANIUM-BASED OXIDES MATERIALS AND THEIR SODIUM-
DOPED DERIVATIVES**

ABSTRACT

Barium titanate (BaTiO_3) and barium nickel titanate ($\text{Ba}_2\text{NiTi}_5\text{O}_{13}$) were synthesized via sol-gel method. Mechanism of formation of BaTiO_3 and $\text{Ba}_2\text{NiTi}_5\text{O}_{13}$ was proposed. The effect of Na doping on structural composition and surface morphology of 3 titanium-based oxides (*i.e.* titanium dioxide (TiO_2), BaTiO_3 and $\text{Ba}_2\text{NiTi}_5\text{O}_{13}$) were investigated. The phase structures of TiO_2 , BaTiO_3 and $\text{Ba}_2\text{NiTi}_5\text{O}_{13}$ *i.e.* anatase, cubic and monoclinic respectively were sustained after Na doping. This indicates that the substitution of Na on Ti atom was a surface phenomenon. The morphology transformation of Na-doped BaTiO_3 particles was observed. Hammett indicator showed that the Na-doped $\text{Ba}_2\text{NiTi}_5\text{O}_{13}$ has the highest basicity. From BET result, the Na-doped $\text{Ba}_2\text{NiTi}_5\text{O}_{13}$ showed the largest specific surface area as compared to Na-doped BaTiO_3 and Na-doped TiO_2 . The application of these titanium-based oxides as the fillers in polyvinyl alcohol (PVA) was investigated. The structural, thermal, electrical and optical properties of these polymer composites were studied. The x-ray diffraction (XRD) and differential scanning calorimetry (DSC) results showed that the polymer composites were semicrystalline with high amorphous region and low T_g values. The 0.3 mol % of Na-doped of PVA/ TiO_2 , PVA/ BaTiO_3 and PVA/ $\text{Ba}_2\text{NiTi}_5\text{O}_{13}$ showed the conductivity of 9.540×10^{-7} , 1.667×10^{-7} and $2.401 \times 10^{-8} \text{ S cm}^{-1}$, respectively. The optical band gaps of PVA based polymer composites showed that they are semiconducting. The optical band gaps were blue shifted when increasing the amount of fillers loading as well as increasing the amount of Na-dopants. The obtained TiO_2 , BaTiO_3 and $\text{Ba}_2\text{NiTi}_5\text{O}_{13}$ and their respective Na-

doped derivatives were also utilized as heterogeneous catalysts for the transesterification of palm cooking oil. Optimal parameters were 5 wt/v % of catalyst loading, oil to methanol volume ratio of 12:1 and 2 hours of reaction at 150 °C. Amongst the catalysts, Na-doped $\text{Ba}_2\text{NiTi}_5\text{O}_{13}$ showed the highest % of methyl esters (ME) yield (96.0 %), whereas TiO_2 showed the lowest (76.3 %). The % of methyl ester (ME) yield is attributed to the basicity and pore size of the respective catalysts.

CHAPTER 1

INTRODUCTION

1.1 A Brief Overview

Titanium-based oxides have attracted interest for a long time. It is because they show interesting properties such as chemical, mechanical, optical, electrical, catalytic, magnetic properties and so on [1]. Titanium-based oxides are semiconductors with large band gap that can only absorb UV light. In order to absorb a wider range of light, titanium-based oxides are doped with alkali metal ions. The electrical and optical properties of the material can then be altered as a result of narrowing the energy band gap. Therefore, a new range of interesting properties can be modified and monitored. Lithium (Li) is commonly used in electrical and optical studies [2]. However, the introduction of sodium (Na) as dopant in polymer composite systems in electrical and optical study is novel. Na^+ is a small ion and its salts readily dissociate into ions after dissolving in solution and interacts with titanium-based oxides. It favors the ions mobility in the material under electrical current and favors the electron excitation after the absorption of photon. For catalytic study, various alkali metal ions are introduced to increase the catalytic activity [3]. The basicity of alkali metal increases from potassium (K) < Na < lithium (Li). Na is chosen for doping because Na is more basic as compared to K. Besides, Na is inexpensive, non toxic and easily available as compared to Li [4]. The synthesis and characterization of titanium-based oxides and their Na-doped derivatives have not much reported. Therefore, the synthesis and characterization of these materials need

to be worked on due to their attractive properties.

In recent years, studies of the various properties such as electrical and optical properties of polymer composites are becoming prevalent due to their applications in electronic devices. Many groups of researchers have study the dispersion of titanium-based oxides into polymer matrix. It has been found that the development of a new material with both polymer and titanium-based oxides properties can be feasible. The properties of polymer composites are mainly dependent on the types of the doping fillers [5]. Electrical and optical properties of polymer composites using titanium-based oxides and their Na-doped derivatives as fillers are still lack of study. Therefore, much work is needed to study the properties of composites for better understanding.

Catalysts have been important in our aspect of live by affecting them tremendously environmentally and economically. The development of titanium-based oxides is related to high stability and multi oxidation state in perovskite crystal structure. These compounds offer excellent for catalytic reactions [6]. Long before, perovskite metal oxides are used in oxidative and reductive catalytic reaction for removal of CO and NO_x from combustion of fuel [7]. In recent years, perovskite metal oxides are studied as potential candidate as a heterogeneous catalyst for biodiesel production [8]. Imminent global shortage of petroleum is now catching attention of researchers in producing sustainable fuel source. Nevertheless, application of titanium-based oxides materials and their Na-doped derivatives as catalysts is still lack of understanding. For this purpose, much work is still needed for this research for better understanding.

1.2 Problem Statements

Titanium-based oxides are traditionally synthesized by solid-state method that requires applying high temperature calcination and high pressure. As a result, the particles formed are found to have rough surfaces and highly agglomerated. Electrical and catalytic properties of materials are therefore can be affected by the surface texture of particles. Therefore, sol-gel chemical method is chosen to be employed. It is because this method can compromise those problems by subsequent application of mild temperature calcinations. In addition, sol-gel method can also control the chemical stoichiometry of the titanium-based oxides.

Despite the limitation of polymer such as low mechanical strength and low thermal stability, applications of polymers are still attracting interest for a long time due to their flexibility in fabrications. Preparation of polymer composites are deemed to be able to overcome the shortcomings by dispersing small amount of titanium-based oxides as fillers in polymer host. The dependence of electrical and optical properties of polymer composites is associated with relative crystallinity of polymer, concentration of fillers, amount of doping, dispersion of fillers *etc.* Polymer composites using various types of polymer as matrix are widely reported. However, polymer composites using titanium-based oxides as fillers are still not widely reported.

Biodiesel production with the application of heterogeneous catalysts is attracting interest recently due to the easy retrievable of the catalysts. Transesterification involves interaction between three different phases (*i.e.* oil/methanol/catalyst). Hence, the catalysts surface condition, surface area, basicity,

pore sizes and doping amount are essential attributes as it provide catalytic sites for transesterification. Although extensive work have been carried out in biodiesel production using various types of metal oxides as heterogeneous catalysts, very few work using titanium-based oxides and their doped derivatives have been reported.

1.3 Research Objectives

Thus, in order to overcome those problems, the objectives of this study are to:

- (i) synthesize and characterize titanium-based oxides (*i.e.* barium titanate, BaTiO_3) and barium nickel titanium oxide ($\text{Ba}_2\text{NiTi}_5\text{O}_{13}$) and Na-doped titanium-based oxides (*i.e.* titanium dioxide (TiO_2), BaTiO_3 and $\text{Ba}_2\text{NiTi}_5\text{O}_{13}$);
- (ii) evaluate and compare the structural, thermal, electrical and optical properties of the respective PVA/titanium-based oxides and PVA/Na-doped titanium-based metal oxides composites thin films; and
- (iii) evaluate and compare the reactivity of the various synthesized titanium-based oxides as heterogeneous catalysts in transesterification of palm cooking oil.

1.4 Scope of Study

This study has been limited to the synthesis of titanium-based oxides (*i.e.* barium titanate (BaTiO_3) and barium nickel titanium oxide ($\text{Ba}_2\text{NiTi}_5\text{O}_{13}$)) via sol-gel synthesis method. The effect of Na-doping on the structural properties of the

perovskite titanium-based oxides is compared with commercial titanium dioxide (TiO₂). Powder x-ray diffraction (XRD) and scanning electron microscopy (SEM) techniques are used to characterize the structural and morphological properties of the titanium-based oxides. The basicity of the titanium-based oxides are determined by Hammett indicator test. The porosity and surface area of the catalysts are characterized via Brunauer-Emmett-Teller (BET) technique.

These 3 titanium-based oxides and their Na-doped derivatives are incorporated with PVA in fabrication of polymer composites thin films. These composites are then characterized for structural, thermal, electrical and optical properties. XRD and Fourier Transform Infrared Spectroscopy (FTIR) is used to study the structural and complexation interaction between PVA and titanium-based oxides. Thermal characteristics of polymer composites such as glass transition temperature (T_g), melting temperature (T_m) and relative crystallinity are determined via differential scanning calorimetry (DSC). Alternating current (AC) electrochemical impedance spectroscopy (EIS) and UV-vis spectrophotometer are employed to determine the AC conductivity and energy band gap of the composites materials respectively.

Lastly, the prepared titanium-based oxides are also employed as heterogeneous catalysts in transesterification study. Gas chromatography (GC) technique is used to determine the % of methyl ester yield of transesterification.

1.5 Thesis Layout

This thesis consists of 7 chapters. The first chapter of the thesis is a general

overview of this work such as problems statements, research objectives and scopes of study of this work. The second chapter of this thesis provides literature review of this work. It covers the development related to this field of study. The third chapter of this thesis discusses the methodology and the technique of characterization of the titanium-based oxides. The fourth chapter of the thesis is focused on discussing the synthesis of BaTiO_3 and $\text{Ba}_2\text{NiTi}_5\text{O}_{13}$. In this chapter, also discussed is the effect of Na-doping on TiO_2 , BaTiO_3 and $\text{Ba}_2\text{NiTi}_5\text{O}_{13}$. In the chapter 5, the characterization of structural, thermal, electrical and optical properties of PVA polymer composites are discussed and compared. The sixth chapter of the thesis discussed the application of the 3 titanium-based oxides and their Na-doped derivatives in transesterification. Lastly, chapter 7 will conclude the overall work and provide future work in this field.

1.6 References

- [1] A.N. Banerjee, "The design, fabrication, and photocatalytic utility of nanostructured semiconductors: Focus on TiO₂-based nanostructures", *Nanotechnology, Science and Applications*, **4**, (2011), 35-65.
- [2] Ch.V.S. Reddy, G.P. Wu, C.X. Zhao, Q.Y. Zhu, W. Chen, R.R. Kalluru, "Characterization of SBA-15 doped (PEO+LiClO₄) polymer electrolytes for electrochemical applications", *Journal of Non-Crystalline Solids*, **353**, (2007), 440-445.
- [3] Z. Yang, W. Xie, "Soybean oil transesterification over zinc oxide modified with alkali earth metals", *Fuel Processing Technology*, **88**, (2007), 631-638.
- [4] L.C. Meher, M.G. Kulkarni, A.K. Dalai, S.N. Naik, "Transesterification of karanja (*Pongamia pinnata*) oil by solid basic catalysts", *European Journal of Lipid Science and Technology*, **108**, (2006), 389-397.
- [5] A. Hassen, A.M. El Sayed, W.M. Morsi, S. El-Sayed, "Influence of Cr₂O₃ nanoparticles on the physical properties of polyvinyl alcohol", *Journal of Applied Physics*, **112**, (2012), 093525-1-093525-8.
- [6] M.A. Peña, J.L.G. Fierro, "Chemical structure and performance of perovskite oxides", *Chemical Reviews*, **101**, (2001), 1981-2017.
- [7] C.H. Kim, G. Qi, K. Dahlberg, W. Li, "Strontium doped perovskites rival platinum catalysts for treating NO_x in simulated diesel exhaust", *Science*, **327**, (2010), 1624-1627.
- [8] M. Misono, "Recent progress in the practical applications of heteropolyacid and perovskite catalysts: Catalytic technology for the sustainable society", *Catalysis Today*, **144**, (2009), 285-291.

CHAPTER 2

LITERATURE REVIEWS

2.1 Overview of Metal Oxides

Metal oxides are a class of materials that has a combination of inorganic metal and nonmetallic (oxygen) components. The bonding interaction strength between metal and oxygen is driven by their electronegativity. It can range from ionic to covalent bonding. Metal oxides are prepared using well refined and highly purified materials [1]. Its attributes of high temperature endurance, mechanical stability and chemical stability properties are attracting interest of many researchers [2]. Metal oxides are the common materials exploited for the wide range of uses such as industrial electrodes [3], catalysts [4-6], electronic components [7, 8], solar cells [9, 10], gas sensors [11], photocatalysts [8, 12], optical materials [8, 13-16], dielectrical materials [17-19], coatings [20], pigments [8] and many more.

2.2 Surface of Metal Oxides

The surface of metal oxides is covered with defects. Point defects (cation vacancies and anion vacancies) are usually responsible for affecting catalytic, optical and electronic properties of a material. Since point defects can modify the properties of the materials, doping is one of the approaches (the other approach is by heating) of controlling the amount of point defects. Therefore, various doping attempts have been reported in literature. Oxygen vacancies are more prominent in metal oxides. If the dopant atoms have valence state less than the doped metal, oxygen has to be removed from the lattice in order to neutralize the overall charge of the material. This is usually

employed in creating more vacancies for controlling certain properties of a material. Chen *et al.* [21] reported the oxygen vacancy in BaTiO₃ that are responsible for conductivity as a result of oxygen diffusion. Besides, Ba_{0.5}Sr_{0.5}Co_{0.8}Fe_{0.2}O_{3-δ} contains oxygen vacancies that can create high ionic mobility in the crystal lattice and has been used as a cathode in fuel cell [3]. Ren *et al.* [22] also reported the potassium-doped BaTiO₃ that increase electrical conduction due to the vacancies.

The surface properties of metal oxides plays an important role in catalysis since catalysis occurs mainly on the surface. The surfaces of metal oxides are covered with M-O ions. These M-O ions are the active sites of catalysts either acidic or basic. Thus, acidity and basicity of metal oxides depend on the surface of metal oxides. The structure of metal oxides is made up of positive metal ions (cations) which behave as electron acceptors are called Lewis acid, and whereas negative oxygen ions (anions) which behave as proton acceptors and are called Brønsted bases. These Lewis acid and Brønsted base phenomenon is due to the unequal distribution of electron sharing in M-O bond. Solid catalyst applies this Brønsted Lewis (solid acid-base theory) to determine the acidity and basicity of the catalyst's surface [23].

Surface of metal oxides is constantly exposed to environment. Therefore, water is easily adsorbed on the surface of metal oxides [23]. Cation acts as Lewis acid and interacts with water molecules is shown in equation (2.1).



Therefore, the resultant metal hydroxide (M-OH) on the surface can act as Brønsted bases or Lewis acid as shown in equation (2.2) and equation (2.3) respectively. The surface condition of heterogeneous catalysts determines the acidity and basicity of the catalysts according to Brønsted-Lewis theory. Given a clean surface of catalysts (no surface -OH), either these acidic or basic sites of catalysts are deemed as catalytic sites as shown in Figure 2.1. Reactants adsorbed on these catalytic sites where catalytic reaction occurs. In methanolysis of oils, it provides sufficient adsorptive sites for methanol, in which the O-H bonds readily break into methoxide anions and hydrogen cations. The methoxide anions then react with triglyceride molecules to yield methyl esters [24]. Hammett indicator test is used to determine the basicity sites of the titanium-based oxides.

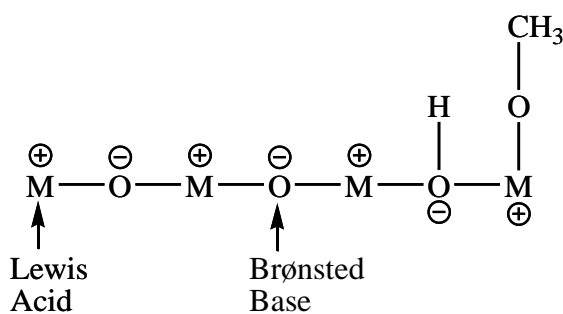


Figure 2.1: Schematic surface of metal oxide catalyst [24].

Furthermore, pores are normally found in the surfaces of metal oxides. These pores are important features for heterogeneous catalysts as it has implications on controlling diffusion and site accessibility of the reactants [25, 26]. Pores are defined as voids between small aggregated particles [25]. Porous structures of materials can be divided into 3 general categories based on their sizes namely, microporous,

mesoporous and macroporous. Microporous materials have pores sizes <2 nm, mesoporous materials have pores sizes in the range of 2-50 nm and macroporous materials have pores sizes >50 nm.

2.3 Titanium-Based Oxides

Titanium-based oxides are the oxides materials that comprise of titanium transition metal ions. Titanium dioxide (TiO_2) is a binary titanium oxide which has 3 crystal phases, (*i.e.* anatase, rutile and brookite). TiO_2 has a wide band gap of 3.2 eV that is suitable to be applied in electronic [7] optical [13, 14] and gas sensing materials [11]. Application of TiO_2 in solar cell is widely reported because of the band gap is in UV-visible range [8, 9]. Furthermore, vanadium doped TiO_2 is studied in order to lower the adsorption in UV and visible light region to achieve photocatalysis for degradation of dye [12]. Beside, TiO_2 is also stable, non toxic and biocompatible so it is suitable to be used as catalysts [6] coatings [20] and pigments [8].

There are various types ternary and quaternary of titanium-based oxides are reported. These types of ternary and quaternary titanium oxides have perovskite crystal structure. Examples of ternary titanium oxides are barium titanate (BaTiO_3) [7, 18, 27-29], lanthanum titanate (LaTiO_3) [30], calcium titanate (CaTiO_3) [31], bismuth titanate ($\text{Bi}_4\text{Ti}_3\text{O}_{12}$) [32], strontium titanate (SrTiO_3) [33] and lead titanate (PbTiO_3) [34]. Beside, there are also quaternary titanium oxides that have been studied. For instance barium nickel titanate ($\text{Ba}_2\text{NiTi}_5\text{O}_{13}$) [35] (Figure 2.2), barium strontium titanate ($\text{Ba}_x\text{Sr}_{1-x}\text{TiO}_3$) [36] and lead zirconate titanate ($\text{Pb}(\text{Zr}_{0.52}\text{Ti}_{0.48})\text{O}_3$) [37] are also studied.

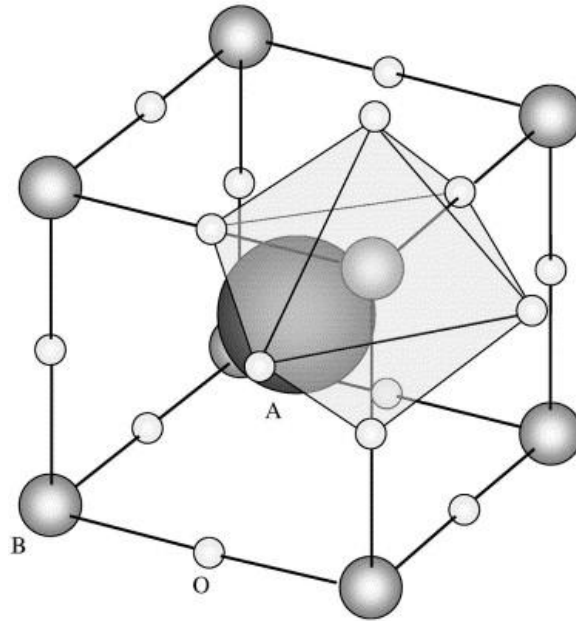


Figure 2.2: Perovskite crystal structure [38].

Perovskite crystal structure has the general chemical formula of ABO_3 and other derivatives of such as $A_2B_6O_{13}$. Certain binary, ternary and quaternary metal oxides that contain 2, 3 and 4 different metal elements also belong to the perovskite-type mixed oxides materials. The fundamental crystal lattice of perovskite structure consists of location of O^{2-} at face centered cube position; larger A atom is located at the center of the lattice and smaller B atom is located at the eight corners position of the lattice as shown in Figure 2.2 [38]. For $BaTiO_3$ perovskite crystal structure, O^{2-} is located at the face side of the crystal structure; Ba^{2+} is a larger ion and is located at the center of the crystal structure and whereas Ti^{4+} ion is smaller and it is located at the eight corners of the crystal structure.

$BaTiO_3$ has two crystal phases, namely tetragonal and cubic. Tetragonal attracted most because of its slight displacement of atoms in crystal structure, and thus is suitable to be applied as dielectrical materials [17, 18, 19]. Because of this distorted

crystal structure of BaTiO₃, it also exhibits piezoelectricity [39], ferroelectricity [40] and ferromagnetic [41] properties that shows varied properties if applied with external pressure, electric and magnetic field, respectively. Besides, BaTiO₃ and PbTiO₃ perovskites also show excellent performance in methane combustion catalysis [42].

2.4 Synthesis Methods for Titanium-Based Oxides

There are many synthesis methods of titanium-based oxides that are reported in literature [4, 5]. Performances and properties of these materials are not only dependent on their purity of materials but also on their surface microstructures. Therefore, choosing synthesis method is important for controlling the crystallinity, morphology and size of the particles and thus affect the physical and chemical properties of the oxides [4, 5]. The synthesis of metal oxides can be divided into two general categories, namely physical method and wet chemical method.

2.4.1 Physical Methods

Physical method is breaking down the bulk precursors by physical means to obtain particles. The drawback of this method is the difficulty in controlling the particle sizes. Solid state milling method is suitable for preparing powder sample [3], whereas physical vapor deposition method is suitable to fabricate thin films [3]. These are two common physical method favored by physicists.

2.4.1.1 Solid State Milling Method

Solid state milling method is a conventional method used to synthesis titanium-based oxides because of its simplicity and low cost practicability. This method uses

ball milling that agitates the mixed precursors. However, eventual exploitation of high temperature of calcinations and pressure condition is harsh for the synthesis of metal oxides [7, 28] as it coarsen the surfaces of particles and cause agglomeration [2]. This is undesirable as agglomerated particles can affect the chemical and physical properties of the particles [5, 43]. BaTiO_3 and $\text{Ba}_2\text{NiTi}_5\text{O}_{13}$ are complex metal oxides, which are synthesized by solid state method conventionally [7, 28, 38]. Adams *et al.* [35] prepared $\text{Ba}_2\text{NiTi}_5\text{O}_{13}$ by mixing required amount of BaCO_3 , NiCO_3 and TiO_2 via solid state milling method. Based on the study, these material exhibits an increased in magnetic moment with increase in temperature that range from 5 to 300 K. It is due to the unpaired electron of Ni that are able to excite to the empty orbital during heating.

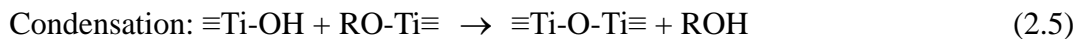
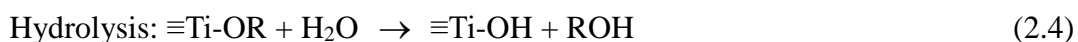
2.4.2 Wet Chemical Methods

Wet chemical methods are introduced to compensate those problems induced by physical methods. There are many wet chemical methods such as sol-gel, hydrothermal, microemulsion and Pechini methods are used to synthesize titanium-based oxides are reported.

2.4.2.1 Sol-Gel Method

Sol-gel method is a method prevalently used to obtain homogeneous, ultrafine titanium-based oxides nanoparticles. Lots of literature has reported the synthesis of titanium-based oxides such as TiO_2 [12, 44], BaTiO_3 [29, 45-47], SrTiO_3 [48], PbTiO_3 [49] via this method. Metal alkoxides and metal chlorides are usually used as the precursor materials, react with water or alcoholic solution leads to the formation of metal hydroxides via hydrolysis process [3]. Repeated inorganic polymerization and

condensation of metal complexes precursors form extended inorganic oxides network. Upon heating, solvent is removed first and subsequent heating lead to the formation of gel. A sol is the dispersion of particles in a medium, whereas, a gel is a polymer of three-dimensional inorganic metal surrounding interconnected pores [3]. Further heat treatment of the gel causes the formation of ultrafine powder of respective metal oxides. Report claimed that the as-prepared particles obtained are amorphous before post heating treatment/calcination by using conventional sol-gel method [12, 50]. The general equations of sol-gel reaction are shown as following equations (2.4) and (2.5) [51]:



The hydrolysis reaction of metal alkoxides with water is a nucleophilic reaction. The mechanism of the reaction involved addition of hydroxide ions ($\text{OH}^{\delta-}$) to the metal complex centers ($\text{M}^{\delta+}$). The positively charged hydrogen is added to alkoxides group followed by removal of alcohol (ROH). Condensation between hydroxides followed by removal of water, thus inorganic network formed. Acid [44, 45]/base [50] catalysts are sometimes added to speed up the hydrolysis reaction. Owing to the highly reactive metal alkoxides towards water requires careful handling in dry atmosphere to avoid rapid hydrolysis and uncontrolled precipitation. A schematic diagram for sol-gel process are presented in Figure 2.3.

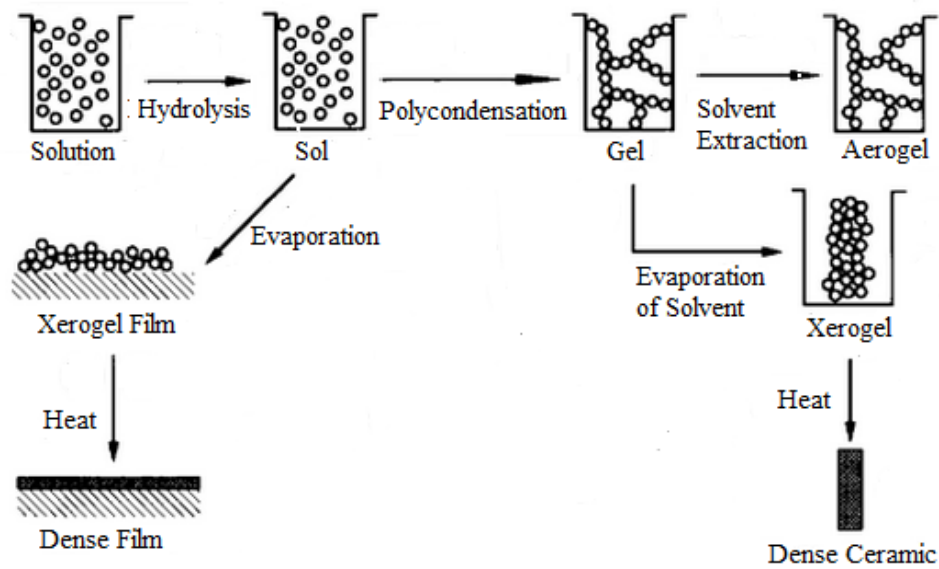


Figure 2.3: Schematic diagram of sol-gel method [52].

Temperature of drying determine whether aerogel or xerogel will be obtained. An aerogel is obtained when the liquid phase is removed under ambient condition, so that the solid network is retained. On the other hand, a xerogel is obtained when the liquid phase is evaporated by extreme drying.

BaTiO₃ thin films are fabricated for miniaturization of electronic component that has high charge storage capability. Thin films deposition of BaTiO₃ on a silicon substrate can also be prepared by sol-gel method [46, 53]. As-prepared sol is dropped on a substrate. Spin coating is then employed in order to disperse the extra sol and to control the thickness of films. The coating is subsequently heated to obtain BaTiO₃ film. Cycles of deposition and heat treatment are sometimes employed to prepare multilayer BaTiO₃ film [46, 53].

Sol-gel method provides several advantages such as requiring low processing cost, providing chemical homogeneity, rather low processing temperature but also can stoichiometrically control the elements of the synthesizing compound.

2.4.2.2 Hydrothermal Method

Hydrothermal method is another commonly used method for preparation of titanium-based oxides particles. For instance, TiO_2 [14] and BaTiO_3 [54] have been prepared via hydrothermal method. High pH value, high temperature and high pressure are applied to the system by using sealed autoclave leading it to supercritical water condition in helping for the dissolution of hardly soluble precursor salts. Synthesis of titanium-based oxides particles are divided into 3 steps including nucleation, growth and aging. Metal oxides are formed after crystallization of nuclei that dissolved in water is shown in Figure 2.4. After the nucleation, the growth of nuclei often leads to form spherical particles which has the lowest surface energy [55]. Controlling the temperature of the system is crucial to obtain the desired shape. Some authors claimed that harsh environment with high temperature, high pressure and alkaline environment resulted aggregation and coarse size of the nanoparticles during aging [28, 56]. Therefore, growth and aging mechanisms are carefully controlled to prevent aggregation of particles.

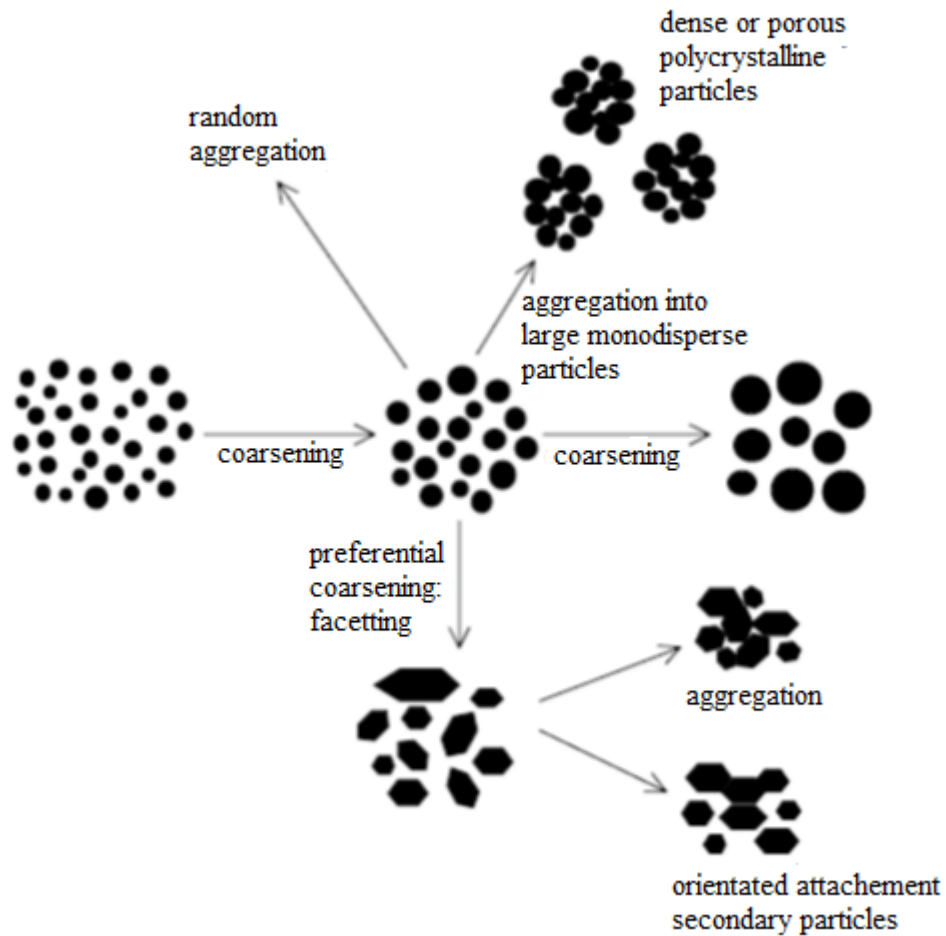


Figure 2.4: Nucleation and growth of particles [55].

2.4.2.3 Water-in-Oil/Microemulsions Method

Titanium-based oxides can also be prepared via microemulsion achieved by reducing metal ions or hydrolysis of metal ions formed prior in the core. The formation of metal oxides happens when reactants exchange between the micelles droplets occurs through the surfactant membrane layer upon collision of two micelles droplets [57]. The nucleation and growth occurred inside the core of microemulsion droplets as shown in Figure 2.5 [58]. Woudenberg *et al.* [57] mixed two separate of barium chloride (BaCl_2) emulsion and titanium tetraisopropoxide ($\text{Ti}(\text{OPr})_4$) emulsion using ethylene-diamino-tetra-acetic acid (EDTA) in a preparation of BaTiO_3 particles.

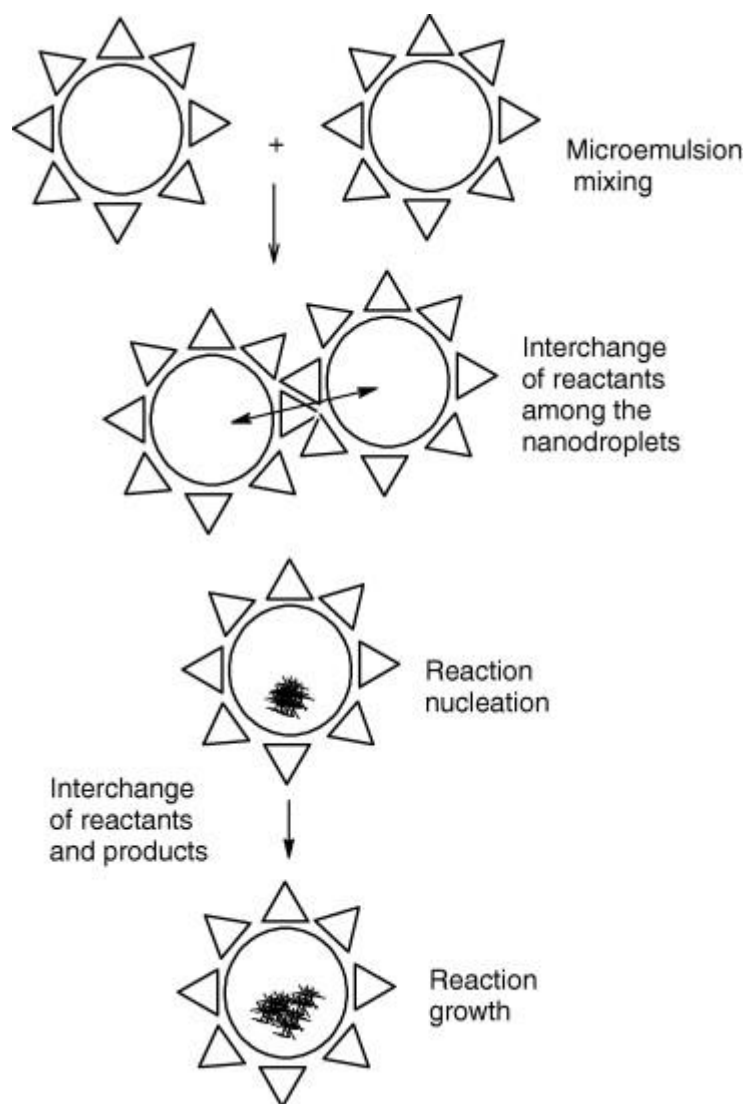


Figure 2.5: Schematic diagram of microemulsion [58].

Microemulsion is a homogeneous phase system which involved stabilizing 2 immiscible phases with the assistance of surfactant. Surfactant such as cetyl-*N,N,N*-trimethylammonium bromide (CTAB) [9] and cetyltrimethylammonium chloride (CTAC) [56, 59] plays an important role in microemulsion by forming micelles. Micelles attracts each other to form an assembly. These micelles' cores are the center of particle formation. The size of particles depends on the micelles' core whereas the shape of particles depends on the alignment of the micelles assembly. Surfactants consists of both hydrophilic head and long hydrophobic tail structure.

Besides, the surfactants also have structure-directing properties that are capable of synthesizing the desired nanostructured materials. Lee *et al.* [9] used CTAB that preferentially adsorbs on particular surfaces of TiO₂ and facilitates the growth of spherical TiO₂ particles. Zhang *et al.* [47] used laurylamine as template to obtain the BaTiO₃ nanorods. Mesoporous BaTiO₃ can also be obtained by using CTAC surfactant [56, 59]. This method is applicable to obtain nanoparticles with desired morphology however total removal of surfactants by calcinations after the incorporation of these surfactants is difficult to achieve [47].

2.4.2.4 Polymerizing-Complexing Sol-Gel Method (Pechini Method)

Combination of citric acid surfactant stabilizer with sol-gel method is known as the Pechini method. This method used citrate salts or mixtures of common salts with citric acids as precursor. This citrate will form complexations via its carboxylate groups with empty orbitals of metals [33, 37]. Because of this, citric acid is well known as a stabilizer in nanoparticles synthesis by functioning as ligand, or acting as a particle surface modifier [5, 60-63]. Although addition of citric acid is able to control particle sizes and shape and dispersion as well as modify the particles morphology, however, it is difficult to be removed [47].

2.5 Polymer-Inorganic Composites

2.5.1 Polymer/Metal or Metal Oxides Composites

Polymer is a high molecular weight molecule with basic repeating units that is called monomer. Polymer composites have received tremendous interest from the last decades. It is because of its wide applications, such as electronic storage, sensor,

optical membranes, coating and many more [64]. Polymer composites consist of a combination of 2 or more different phases of constituents. Polymer has long-term stability, lightweight and flexible for various designs, but they have low temperature endurance and low mechanical strength. At past, various combination of polymer matrix phase and fillers composites is introduced to complement or enhance the properties of one another for the specific application.

The toughness property of metal oxides enhance the mechanical property of polymer. For instance, clay is dispersed in rubber to reinforce the polymer matrix [58]. The antimicrobial behavior of polymer composite is attributed to the incorporation of the noble metal. Food packaging that uses silver (Ag) and polyethylene composites reaches 99.99 % antimicrobial efficiency against *Escherichia Coli* bacteria [65]. Furthermore, the electronic and catalytic of metal oxides can add to the polymer properties such as the processability and the film-forming capability. Lithium manganese oxide (LiMn₂O₄)-polypyrrole composite cathode is applied for lithium rechargeable battery [66]. Noble metal platinum (Pt) incorporated in poly(4-vinylpyridine) is studied for catalytic hydrogenation applications [67]. Besides, the addition of conducting metal oxides can enhance the electrical conductivity of natural polymer. Semiconducting Co₃O₄ dispersed in biodegradable chitosan shows conductivity as high as $1.940 \times 10^{-2} \text{ S cm}^{-1}$ at room temperature [68].

2.5.2 Polymer/Titanium-Based Oxides Composites

The types of fillers that are incorporated can enhance and complement the overall properties of polymer composites. Fillers such as titanium-based oxides have high thermal and electrical conductivity, ductility and strength, but brittle. Thus, at past,

many different combination of polymer matrix phase and titanium-based metal oxides fillers nanocomposites have been prepared for the specific application.

For instance, cellulose /TiO₂ nanocomposite is used to fabricate biosensor [69]. TiO₂ incorporated in polyaniline is studied for photocatalytic in degradation of methyl orange dye applications [70]. Besides, cellulose/TiO₂ coating is also studied for corrosion resistance [20]. Poly(3-dodecylthiophene)/TiO₂ nanocomposite is studied for solar cell application [8, 10] while polyaniline/TiO₂ is applied in CO gas sensor [11].

Polyvinylpyrrolidone/BaTiO₃ [19], polyaniline/BaTiO₃ [71] and polyvinylidene fluoride/BaTiO₃ [72] nanocomposite thin films is studied for dielectric properties. Polystyrene/barium strontium titanate shows good thermal properties [73]. Polyaniline/Li₄Ti₅O₁₂ is studied for their electrochemical process and applied in electrode material [74]. Polypyrrole/lithium manganese oxide (LiMn₂O₄) composite cathode is applied for lithium rechargeable battery [66]. Thermal behavior of polyvinylidene fluoride/barium strontium titanate is studied [75]. In all the cases, nanocomposites have the advantages of improving functionality and properties given by combination of both individual components of polymer and oxides.

2.5.3 PVA/Titanium-Based Oxides Composites

Polyvinyl alcohol (PVA) is a water-soluble polymer contains functional group of hydroxide –OH attached to the backbone of carbon chain. PVA is a semicrystalline polymer and therefore it contains the amorphous region that promotes the mobility of ion. The chemical structure of PVA is shown in Figure 2.6. Its –OH groups are able to form complexes with incorporated metal oxides and form composites. Besides, this

polar polymer has charge storage capacity and high dielectrical strength [76].

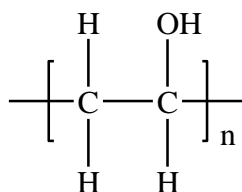


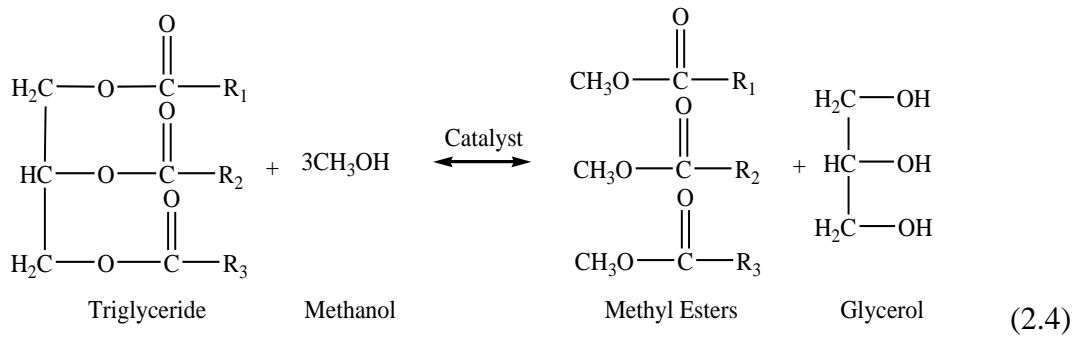
Figure 2.6: Chemical structure of PVA.

PVA composites containing various titanium-based fillers are reported for various applications. For instance, Khanna *et al.* [77] synthesize TiO₂ with particle sizes of 2.3 nm and prepare PVA/TiO₂ composites that show photoluminescence (PL) emission at 330 nm. Liu *et al.* [78] prepare PVA/TiO₂ nanocomposite films for photocatalytic degradation of methyl orange. It is found that the dielectric, mechanical and thermal properties of PVA improved with addition of BaTiO₃ filler which is suitable for capacitor application [79]. On the other hand, composites with other titanium-based oxides fillers such as PVA/lead titanate [80] and PVA/barium zirconium titanate [81] are studied for improving its dielectric properties.

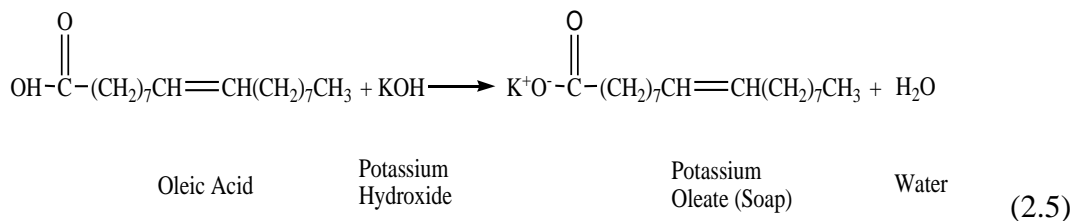
2.6 Applications of Titanium-Based Oxides

2.6.1 Catalysts for Transesterification

Transesterification is the catalytic reaction of converting triglycerides to fatty acid methyl esters (FAME) by using methanol. The reaction of the transesterification is shown in equation (2.4).



This reaction is also known as alcoholysis; if methanol is used as alcohol in the reaction, methanolysis can also be known. The resulting methyl esters are utilized as biodiesel. Diverse variety of oil feedstock have been studied and are utilized in biodiesel production. Examples are vegetable oils [82-88], animal oils [89] or waste oils [90]. Vegetable oils are commonly used because of low free fatty acid content ($\leq 0.1\%$) and low water content ($\leq 0.1\%$) as compared to animal oil. If oils feedstock contains free fatty acid (FFA) such as oleic acid, base catalyst will react with oleic acid to produce soap as shown in equation (2.5) [91]. This side reaction is undesirable because this will deactivate catalyst, reduce ME yield and besides the soap production will make purification process troublesome [91].



On the other hand, high water content can also affect ME yield. High water content can produce soap (saponification). Water reacts with triglycerides to produce diglyceride and fatty acid as shown in equation (2.6).